

## PARAMETERS TO MODEL CARTILAGE AS OSTEOARTHRITIS PROGRESSES

Xiaogang Wang (1), David M. Pierce (1,2)

(1) Department of Mechanical Engineering, University of Connecticut, Storrs, CT, USA  
(2) Department of Biomedical Engineering, University of Connecticut, Storrs, CT, USA

### INTRODUCTION

The remarkable mechanical function of healthy cartilage derives from interactions among proteoglycans, networked collagens (in three through-thickness zones: superficial, middle, and deep), and electrolytic fluid. Osteoarthritis (OA) is a pervasive disease involving failure of the synovial joint and deleterious changes in composition and micro-structure (e.g. loss of zones) of cartilage. Changes in cartilage properties correlate with tissue composition and thus with OA severity [1-3].

During normal movement, healthy cartilage provides load transfer between bones and near-frictionless joint articulation, compressing as much as 30% under pressures up to 20 MPa [1,4,5]. These large *in vivo* deformations of the tissue, where shear is critical in both failure and cell death, mean mechanical analyses of cartilage should employ large-strain, nonlinear mechanics. Moreover, research shows tensile properties of the collagen network dominate the shear response [1,6].

Finite element (FE) modeling plays a well-established and increasingly significant role in analyses of cartilage at organ, tissue, and cell scales. An accurate FE model requires an experimentally calibrated and validated constitutive model; however, research literature features few calibrated large-strain constitutive models for healthy human cartilage, and even fewer for osteoarthritic human cartilage [2,3].

We established a finite-strain constitutive model of cartilage addressing both solid (reinforcement) and fluid (permeability) dependence on the network of collagen fibers, and which admits patient-specific organizations of collagen via diffusion tensor MRI [7]. We also included osmotic swelling and the osmotically prestretched/prestressed state of cartilage determined from medical images [8]. In this study, we aimed to advance our constitutive model by leveraging our novel experimental data [9,10] to establish parameters with respect to structurally defined OA progression quantified by OARSI scoring [11].

### METHODS

*Experimental Evidence.* We previously harvested 106 3×3 mm, full-thickness specimens of healthy and progressively osteoarthritic

cartilage from 17 donors [9,10]. Using standard histological scoring we determined the OARSI grade of each specimen [11]. Briefly, we applied cyclic simple-shear displacements at a rate of 75 μm/min for six cycles, and at maximum displacements corresponding to shear strains of 5%, 10%, 15%, 20%, and 25%. Many mechanical tests failed at 20% shear strain and we used data only up to 15%. We grouped specimens based on OARSI grade: Healthy ( $n = 42$ ) contains healthy specimens with OARSI score of 0-1; OARSI-1 ( $n = 11$ ) with OARSI grade  $\in [0,2)$ ; OARSI-2 ( $n = 20$ ) with OARSI grade  $\in [2,3)$ ; OARSI-3 ( $n = 17$ ) with OARSI grade  $\in [3,4)$ ; and OARSI-4 ( $n = 10$ ) with OARSI grade  $\geq 4$ .

*Constitutive Model.* We described cartilage as a biphasic continuum  $\varphi = \varphi^S + \varphi^F$  of a porous solid phase  $\varphi^S$  saturated with a fluid phase  $\varphi^F$ . We calculated the total Cauchy stress as [7,8]

$$\boldsymbol{\sigma} = -p\mathbf{I} + 2\rho^S \mathbf{F}_S \frac{\partial \Psi^S}{\partial \mathbf{C}_S} \mathbf{F}_S^T = -p\mathbf{I} + \boldsymbol{\sigma}_E^S, \quad (1)$$

where  $p$  is the fluid pressure,  $\mathbf{I}$  is the identity,  $\rho^S$  is the partial density of solid,  $\mathbf{F}_S$  is the solid deformation gradient,  $\mathbf{C}_S = \mathbf{F}_S^T \mathbf{F}_S$ , and  $\boldsymbol{\sigma}_E^S$  is the effective Cauchy stress. We used an additive decomposition of the solid Helmholtz free-energy  $\Psi^S$  into contributions from Donnan osmotic pressure  $\Psi_{OP}^S$ , an isotropic matrix  $\Psi_{IM}^S$ , and a fiber network  $\Psi_{FN}^S$  as [8]

$$\Psi^S = \Psi_{OP}^S(J_S) + (1 - \nu)\Psi_{IM}^S(J_S, I_1) + \nu\Psi_{FN}^S(\mathbf{C}_S), \quad (2)$$

where  $J_S = \det \mathbf{F}_S$ ,  $\nu$  is the volume fraction of collagen to total solid, and  $I_1 = \text{tr} \mathbf{C}_S$ . We modeled the Cauchy stress from osmotic pressure as

$$\boldsymbol{\sigma}_{OP}^S = -R\Theta \left[ \sqrt{4(\bar{c}_m)^2 + (c_m^{fc})^2} - 2\bar{c}_m \right] \mathbf{I}, \quad (3)$$

where  $R = 8.314 \times 10^3 \text{ J}/(\text{K} \cdot \text{mol})$ ,  $\Theta$  is the absolute temperature,  $\bar{c}_m$  is the ion concentration of the external solution, and the concentration of the fixed charge depends on the deformation as [8]

$$c_m^{fc} = c_{OS}^{fc} (1 - n_{OS}^S) (J_S - n_{OS}^S)^{-1}, \quad (4)$$

where  $c_{OS}^{fc}$  is the initial concentration of fixed charge (within the tissue) and  $n_{OS}^S$  is the initial solid volume fraction. We modeled the (largely)

proteoglycan solid matrix  $\Psi_{IM}^S$  using a neo-Hookean function extended with compaction effects. We modeled the dispersed network of collagen  $\Psi_{IM}^S$  using an orientation distribution function calibrated with diffusion tensor MRI. We considered the viscoelasticity of both the proteoglycan and collagen solids using two parameters:  $\beta$  [-], a magnitude factor, and  $\tau$  [s] the associated relaxation time, cf. [12].

**Inverse Finite Element Analyses.** We modeled the center slice of specimens under plane strain (**Fig. 1(a)**) using 20-node hexahedral elements to simulate the shear tests in FEBio (U. of Utah). We validated our mesh, using an  $h$ -refinement test [9,12]. In light of the available data we leveraged previous studies to establish some of the parameters (**Table 1**). We started the parameter optimization using a homogeneous constitutive model where we used  $z^* = 0.5$  to obtain the averaged parameters and the diffusion tensor  $\mathbf{D} = \mathbf{I}$  for an isotropic distribution of fibers. With this model we optimized the fiber stiffness parameter  $k_1 \in [0.3, 10]$ , initialized with  $k_1 = 3.0$ , using the “interior-point” algorithm. For healthy samples, we then fitted a heterogeneous model consisting of a superficial zone (SZ, 15%), middle zone (MZ, 55%), and deep zone (DZ, 35%) based on the tissue thickness (**Fig. 1(b)**) to refit  $k_1$ . To investigate the contribution of prestress resulting from Donnan osmotic pressure we repeated the parameter optimization without osmotic pressure and without the backward displacement method (BDM) to determine initial equilibrium [8].

**Statistical Analyses.** We tested whether the fitted  $k_1$  was normally distributed by the Jarque-Bera test. We used the two-sample  $t$ -test to establish if two data sets were significantly different (with  $p = 0.05$ ).

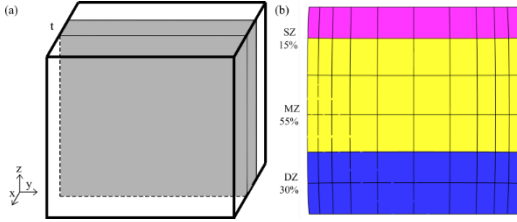


**Figure 1: FE model of the shear experiment: (a) schematic with center slice in plane strain; (b) mesh with three distinct zones.**

**Table 1: Model parameters from previous studies, where  $z^* \in [0, 1]$  is the normalized tissue thickness (zero refers to the articular surface and one to the interface with subchondral bone) [7,8].**

Parameter	Value	Unit
$\Theta$	310	K
$\mu$	0.23	MPa
$k_2$	8.0	—
$\beta_{IM}, \beta_{FN}$	2.7, 1.5	—
$\tau_{IM}, \tau_{FN}$	360, 1500	s
$c_{OS}^{fc}$	$2.0 \times 10^{-7}$	mol/mm <sup>3</sup>
$\bar{c}_m$	$1.5 \times 10^{-7}$	mol/mm <sup>3</sup>
$n_{OS}^S(z^*)$	$0.15 + 0.15(z^*)$	—
$v(z^*)$	$0.43(z^*)^2 - 0.60(z^*) + 0.85$	—
$f_{cp}^S(z^*)$	$0.36 + 0.11(z^*)$	—
$k_{OS}(z^*)$	$(1 - 0.9(z^*)) \times 10^{-3}$	mm <sup>4</sup> /(N · s)
$m(z^*)$	$3.0 + 5.0(z^*)$	—

## RESULTS

Fitting results of the healthy samples with both homogeneous and heterogeneous models are normal distributed. There is no significant difference between the bulk responses of the two models with the BDM approach. Without osmotic pressure and BDM, the optimal fiber stiffness parameter  $k_1$  is larger in the homogeneous model (**Fig. 2(a)**). Starting from OARSI-1,  $k_1$  decreased as OARSI grade increased. The most significant changes occurred between OARSI-1 and OARSI-2 in

both BDM and Non-BDM approaches. Since OARSI-3 in BDM and OARSI-4 in both BDM and Non-BDM did not pass the JB-test, we show median and interquartile ranges for these three cases instead of mean and standard deviation (**Fig. 2(b)**). We also plot the bulk stress-strain response of representative specimens for comparison (**Fig. 3**).

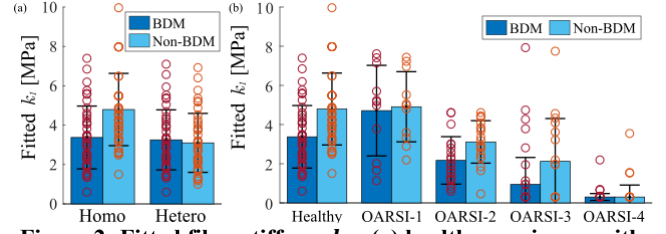


**Figure 2: Fitted fiber stiffness  $k_1$ : (a) healthy specimens with different methods and models, (b) specimens from OARSI grades.**

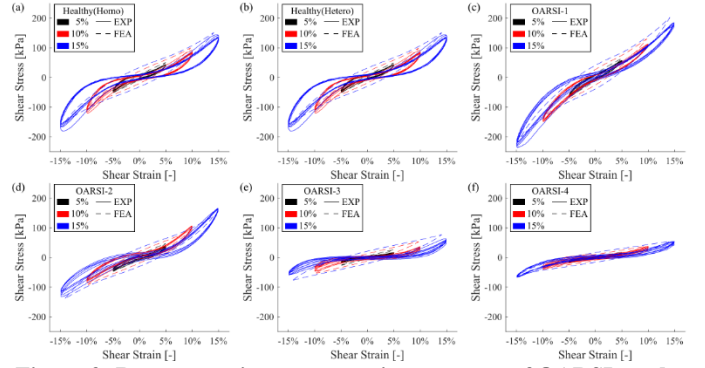


**Figure 3: Representative stress-strain responses of OARSI grades.**

## DISCUSSION

In this study, we calibrated our constitutive model with experimental data from healthy and progressively osteoarthritic human articular cartilage undergoing large-strain shear. Since many of the parameters we require are directly measurable and well established (e.g. the permeability of healthy cartilage) we focused our fitting under shear on the stiffness of collagen fibers, particularly since the properties of the collagen network dominate the shear response of cartilage. With advancing OA, the fiber stiffness parameter  $k_1$  progressively reduces indicating progressive loss of collagen integrity. We can further improve our cartilage model by leveraging more experimental data.

We also established a general method to better calibrate our cartilage model using experimental data. Our methods can be expanded for fitting multiple parameters simultaneously or different constitutive models, or leveraging other types of experimental data. With our models and modeling methods, we hope to improve the fidelity of FE-based, patient-specific biomechanical simulations of joints and cartilage.

## ACKNOWLEDGEMENTS

NSF CAREER 1653358, NSF 1662429; N. Kamath, F. Maier.

## REFERENCES

- [1] Mow, VC et al., *Basic Orthopaedic Biomechanics & Mechano-Biology*, 181-258, 2005.
- [2] Robinson, DL et al., *J Mech Beh Biomed Mat*, 61:96-109, 2016.
- [3] Nissinen, MT et al., *J. Biomech*, 126:110634, 2021.
- [4] Park, S et al., *J. Biomech.*, 36:1785-1796, 2003.
- [5] Bingham, JT et al., *Rheum*, 47:1622-1627, 2008.
- [6] Mow, VC et al., 1992.
- [7] Pierce, DM et al., *Biomech Model Mechno*, 15:229-244, 2016.
- [8] Wang, X et al., *J Mech Beh Biomed Mat*, 86:409-422, 2018.
- [9] Maier, F et al., *J Mech Beh Biomed Mat*, 65:53-65, 2017.
- [10] Maier, F et al., *Osteoarthritis Cartilage*, 27:810-22, 2019.
- [11] Pritzker, KPH. et al., *Osteoarthritis Cartilage*, 14:13-29, 2006.
- [12] Wang, X. et al., *J Mech Beh Biomed Mat*, 104:150, 2020.